Weyl-Heisenberg Framework-Based Orthogonal Waveform Design for Doubly Selective Channels

Zhuangzhuang Liao*†, Xiaojie Fang*, Lizhe Liu‡, Xuejun Sha*, and Dirk Slock†
*Harbin Institute of Technology, Harbin, China
†Communication Systems Department, Eurecom, Biot, France
‡National Key Laboratory of Advanced Communication Networks, Shijiazhuang, Hebei, China
Email: {Liao.Zhuangzhuang, Dirk.Slock}@eurecom.fr, liu_lizhe@sina.com, {fangxiaojie, shaxuejun}@hit.edu.cn

***Abstract*—This paper proposes a unified waveform design framework for doubly selective channels based on the Weyl-Heisenberg (WH) group. By linking waveform orthogonality to the ambiguity function and its zero set under unitary time-frequency shift operators, the proposed framework unifies SC-FDE, OFDM, OTFS, and AFDM as different operator paths on the delay-frequency-shift grid. Within this framework, we further design a novel WH-based waveform with a constant-modulus prototype in both the time and frequency domains, yielding orthogonal basis signals with near-uniform time-frequency energy spreading. In doubly selective channels, this waveform exhibits BER performance close to the theoretical minimum mean-square error (MMSE) lower bound.**

I. Introduction

Since 2019, the commercial rollout of fifth-generation (5G) systems has substantially improved peak data rates and reliability while reducing latency. Along with the evolution of 5G, researchers have turned their attention to the sixth-generation (6G) mobile communication systems. In the white paper "Framework and overall objectives of the future development of IMT for 2030 and beyond" published by ITU-R [1], one of the key visions for 6G is to further enhance the communication performance of 5G while integrating diverse functionalities of communication signals into the 6G architecture, thereby empowering emerging vertical applications such as industrial Internet, vehicular networks, high-speed railway communications, and unmanned aerial vehicle (UAV) communications [2], [3].

Most of the above requirements are associated with higher mobility and larger transmission bandwidths. In such scenarios, multipath delay spread and Doppler spread render the channel doubly selective, inducing frequency-selective and time-selective fading simultaneously. Conventional waveforms such as orthogonal frequency-division multiplexing (OFDM) and single-carrier transmission with frequency-domain equalization (SC-FDE) primarily address one dimension of selectivity and may therefore suffer noticeable performance degradation in doubly selective channels.

In recent years, several new modulation schemes tailored to doubly selective channels have been proposed. Representative examples include orthogonal time-frequency space (OTFS), which maps symbols to the delay-Doppler domain to better capture doubly selective channel dynamics, and affine frequency-division multiplexing (AFDM), which uses affine Fourier transforms to reshape signal energy in the time-frequency plane [4], [5]. Although these schemes have shown promising performance in specific scenarios, their analyses rely on different mathematical formalisms, making it difficult to reveal connections, compare structures, and derive reusable design rules across waveforms. Related formulations based on orthogonal short-time Fourier (STF)/Gabor or Weyl-Heisenberg (WH) signaling have also been studied for communications over doubly selective channels. In particular, Han and Zhang investigated multicarrier transmission via WH frames over time-frequency dispersive channels, with emphasis on pulse shaping, lattice design, and signaling over WH-generated waveform sets [6]. More recently, Gopalam developed a general delay-Doppler signaling framework based on periodic discrete WH sets and prototype ambiguity functions, covering time-division multiplexing (TDM)-like / frequency-division multiplexing (FDM)-like signaling, Zak-OTFS, and chirped WH-based constructions [7]. These studies further highlight the relevance of WH/STF-based formulations for waveform analysis and design over doubly selective channels.

Motivated by these observations, this paper develops a unified waveform design framework for doubly selective channels from the Weyl-Heisenberg perspective. By modeling time and frequency shifts as unitary WH operators and characterizing orthogonality via the discrete ambiguity function and its zero set, the framework offers a common interpretation of SC-FDE, OFDM, OTFS, and AFDM as different operator paths on the delay-frequency-shift grid. Guided by the framework, we further propose a novel WH-based waveform with a constant-modulus prototype in both the time and frequency domains, yielding orthogonal basis signals with near-uniform time-frequency energy spreading. Similar to OTFS and AFDM, it approaches the MMSE BER lower bound in doubly selective channels.

Notation: Bold lowercase and uppercase letters denote vectors and matrices, respectively. $(\cdot)^{\mathrm{T}}$ and $(\cdot)^{\mathrm{H}}$ denote transpose and Hermitian transpose, respectively. $\mathrm{diag}(\cdot)$ forms a diagonal matrix. $\otimes$ denotes the Kronecker product. $\mathrm{mod}(\cdot, N)$ denotes modulo-N reduction and $\lfloor \cdot \rfloor$ denotes the floor operator. $\mathrm{vec}(\cdot)$ stacks the columns of a matrix into a vector, and $\mathrm{vec}_{\mathrm{row}}(\cdot)$ denotes row-wise vectorization.

II. Mathematical Meaning of the Weyl-Heisenberg Group in Communications

The Weyl-Heisenberg group is a fundamental mathematical structure in quantum mechanics and harmonic analysis. In communications, it captures the algebra of time shifts and frequency modulations.

For a signal $s(t)$, consider the two elementary operations: a time shift $s(t-\tau)$ and a frequency shift $e^{2\pi \mathrm{j}\upsilon t}s(t)$. The Weyl-Heisenberg group is precisely the mathematical structure generated by these two basic operations and all their combinations. It is important to note that the time-shift and frequency-shift operations do not commute. The order in which they are applied matters.

The Weyl-Heisenberg group $\mathbb{H}$ can be defined on the real domain $\mathbb{R}$ (continuous-time case) or on the integers $\mathbb{Z}$ (discrete-time case). The continuous Weyl-Heisenberg group $\mathbb{H}$ is the set $\mathbb{R} \times \mathbb{R} \times \mathbb{T}$, where $\mathbb{T} = \{z \in \mathbb{C} : |z| = 1\}$ is the unit circle in the complex plane. It is equipped with the following group operation:

$$\begin{aligned}&(\tau_1, \upsilon_1, z_1) \circ (\tau_2, \upsilon_2, z_2)\\&= \left(\tau_1 + \tau_2,\ \upsilon_1 + \upsilon_2,\ z_1 z_2 e^{2\pi \mathrm{j}\upsilon_1 \tau_2}\right),\\&\forall \left(\tau_1, \upsilon_1, z_1\right), \left(\tau_2, \upsilon_2, z_2\right) \in \mathbb{H}.\end{aligned} \tag{1}$$

Here $\tau \in \mathbb{R}$ denotes the time-shift parameter, $\upsilon \in \mathbb{R}$ denotes the frequency-shift (modulation) parameter, and $z \in \mathbb{T}$ is a global phase factor with unit magnitude. This factor is crucial in quantum mechanics, but in communication applications it does not affect signal energy or orthogonality and can therefore be ignored or set to one. The pair $(\tau_1 + \tau_2, \upsilon_1 + \upsilon_2)$ in the result represents the addition of shift parameters, while the third factor $e^{2\pi \mathrm{j}\upsilon_1\tau_2}$ is a nontrivial phase term that reflects the non-commutativity of time and frequency shifts.

We focus on a unitary representation of this group on the signal space $L^2(\mathbb{R})$, which preserves inner products.

We define two basic unitary operators.

Time-shift operator:

$$(T_\tau s)(t) = s(t-\tau), \tag{2}$$

which shifts the signal $s(t)$ along the time axis by τ.

Frequency-shift operator:

$$(M_\upsilon s)(t) = e^{2\pi \mathrm{j}\upsilon t}s(t), \tag{3}$$

which modulates the signal $s(t)$ by the complex exponential with frequency υ.

Based on these two basic unitary operators, we can define a unitary representation Θ of the Weyl-Heisenberg group, which maps each element of $\mathbb{H}$ to a unitary operator acting on $L^2(\mathbb{R})$:

$$\Theta(\tau, \upsilon, z) = z \cdot T_\tau M_\upsilon. \tag{4}$$

For any signal $s(t) \in L^2(\mathbb{R})$, we have

$$\big(\Theta(\tau, \upsilon, z)s\big)(t) = z \cdot e^{2\pi \mathrm{j}\upsilon(t-\tau)}s(t-\tau), \tag{5}$$

which performs a time shift, a frequency modulation, and multiplies by a global phase.

The time-shift and frequency-shift operators of the Weyl-Heisenberg group satisfy the Heisenberg relation

$$M_\upsilon T_\tau = e^{2\pi \mathrm{j}\upsilon\tau} T_\tau M_\upsilon. \tag{6}$$

In digital communication systems, we deal with discrete time and discrete frequency. Hence, we use a discrete subgroup of the Weyl-Heisenberg group. Fix a time spacing Δt and a frequency spacing Δf (e.g., the subcarrier spacing). The discrete subgroup is then generated by elements $(k\Delta t, l\Delta f, 1)$, where $k, l \in \mathbb{Z}$. The corresponding discrete Weyl-Heisenberg operator is

$$\big(\Theta(k\Delta t, l\Delta f, 1)s\big)(t) = e^{2\pi \mathrm{j}l\Delta f(t-k\Delta t)}s(t-k\Delta t). \tag{7}$$

When both the time-shift operator T and the frequency-shift operator M are represented in matrix form, their actions in an N-dimensional discrete signal space can be written as

$$T_k = \mathbf{\Pi}^k, \qquad M_l = \mathrm{diag}\left(e^{\mathrm{j}\frac{2\pi lm}{N}}\right)_{m=0}^{N-1}, \tag{8}$$

where $\mathbf{\Pi}$ denotes the cyclic shift matrix. They satisfy the discrete Heisenberg commutation relation

$$M_l T_k = e^{\mathrm{j}\frac{2\pi kl}{N}} T_k M_l. \tag{9}$$

Each element of the discrete Weyl-Heisenberg group is thus a combination of time shift and frequency modulation, together with a global phase:

$$\Phi_{k,l,\phi} = e^{\mathrm{j}\phi} T_k M_l, \quad k, l \in \{0, 1, \ldots, N-1\},\ \phi \in \mathbb{R}. \tag{10}$$

Ignoring the global phase, the discrete Weyl-Heisenberg group has N^2 distinct elements.

III. Design of Orthogonal Communication Systems Based on the Weyl-Heisenberg Group

A. Mathematical Theory

A family of waveforms of the form

$$\left\{g_{k,l}(t) = e^{2\pi \mathrm{j}l\Delta f(t-k\Delta t)}g(t-k\Delta t)\right\}, \quad k, l \in \mathbb{Z}, \tag{11}$$

is called a Gabor frame or Weyl-Heisenberg frame, where $g(t)$ is a prototype waveform [8], such as a Gaussian pulse or a rectangular pulse. If Δt and Δf satisfy $\Delta t \cdot \Delta f = 1$, then for a suitable choice of $g(t)$ the set $\{g_{k,l}(t)\}$ can form an orthonormal basis of $L^2(\mathbb{R})$.

For a discrete waveform vector $g(n)$ of length N, to construct an N-dimensional orthogonal communication system using the operators T and M, we need to find N pairwise orthogonal vectors. From the perspective of the Weyl-Heisenberg group, the search for such orthogonal vectors can be carried out by examining the zeros of the ambiguity function of the signal.

The ambiguity function of a signal $g(t)$ is defined as

$$\chi(\tau, f) = \int_{-\infty}^{\infty} g(t)g^*(t-\tau)e^{-\mathrm{j}2\pi f(t-\tau)}\,\mathrm{d}t. \tag{12}$$

Its discrete form can be written as

$$r(k, l) = \sum_{n=0}^{N-1} g(n)g^*\big(\mathrm{mod}(n-k, N)\big)e^{-\mathrm{j}2\pi\frac{(n-k)l}{N}}, \tag{13}$$

where $g(n)$ is an N-length discrete signal, k is the delay index, and l is the frequency-shift index. The value $r(k,l)$ is the ambiguity-function value at delay k and frequency shift l.

A "zero" of the ambiguity function refers to a point where the magnitude $|r(k,l)|$ is zero. At such delay-frequency-shift combinations, the signal is orthogonal to its own time- and frequency-shifted version, and thus exhibits good resolution properties.

Proposition: For any discrete signal $g(n)$, under the action of elements of the discrete Weyl-Heisenberg group, the ambiguity function changes only by a global phase factor and thus its zero set remains invariant.

Proof: The ambiguity function in matrix form can be written as

$$\begin{aligned} r(k,l) &= \left(T_k M_l g\right)^{\mathrm{H}} g \\ &= g^{\mathrm{H}} M_l^{\mathrm{H}} T_k^{\mathrm{H}} g. \end{aligned} \tag{14}$$

Let $\bar{g}(n)$ be the signal obtained by applying the operator $T_p M_q$ to $g(n)$. Denote the ambiguity function of $\bar{g}$ by $r_{p,q}(k,l)$, then

$$\begin{aligned} r_{p,q}(k,l) &= \left(T_k M_l \bar{g}\right)^{\mathrm{H}} \bar{g} \\ &= \left(T_k M_l T_p M_q g\right)^{\mathrm{H}} T_p M_q g \\ &= g^{\mathrm{H}} M_q^{\mathrm{H}} T_p^{\mathrm{H}} M_l^{\mathrm{H}} T_k^{\mathrm{H}} T_p M_q g. \end{aligned} \tag{15}$$

Using the discrete Heisenberg commutation relation to exchange the order of T and M, together with $T_p T_p^{\mathrm{H}} = \mathbf{I}$ and $M_q M_q^{\mathrm{H}} = \mathbf{I}$, we obtain

$$r_{p,q}(k,l) = e^{\mathrm{j}\phi} g^{\mathrm{H}} M_l^{\mathrm{H}} T_k^{\mathrm{H}} g, \tag{16}$$

for some real phase ϕ. Thus $r_{p,q}(k,l)$ differs from $r(k,l)$ only by a phase factor, and their zero sets coincide. □

Based on this result, we can construct orthogonal communication systems from a prototype waveform $g(n)$ as follows. We first compute the zeros of the ambiguity function of $g(n)$ and plot them on the delay-frequency-shift grid. Then we select an index set such that the modulo differences between any two points lie in the ambiguity-function zero set. In this paper, we refer to the corresponding operator index set used to build an orthogonal basis from a given prototype waveform as the "path".

For any two waveforms $g_{k_1,l_1}(n)$ and $g_{k_2,l_2}(n)$ on the path, orthogonality is equivalent to

$$\left(T_{k_1} M_{l_1} g\right)^{\mathrm{H}} T_{k_2} M_{l_2} g = g^{\mathrm{H}} M_{l_1}^{\mathrm{H}} T_{k_1}^{\mathrm{H}} T_{k_2} M_{l_2} g = 0. \tag{17}$$

Using the Heisenberg relation, together with $T_p T_p^{\mathrm{H}} = \mathbf{I}$, $M_q M_q^{\mathrm{H}} = \mathbf{I}$, $T_p T_k = T_{p+k}$ and $M_q M_l = M_{q+l}$, this can be rewritten as

$$g^{\mathrm{H}} M_{l_1-l_2}^{\mathrm{H}} T_{k_1-k_2}^{\mathrm{H}} g = 0. \tag{18}$$

If, for any two grid points (k_1,l_1) and (k_2,l_2) on the selected path, their modulo difference

$$\left(\mathrm{mod}(k_1-k_2,N),\, \mathrm{mod}(l_1-l_2,N)\right)$$

still lies in the zero set of the ambiguity function, then the waveform set generated along this path is pairwise orthogonal.

A simple example is a straight-line path, which can be defined as

$$\mathcal{P}_i = T_{pi} M_{qi}, \tag{19}$$

whose slope on the delay-frequency-shift grid is p/q.

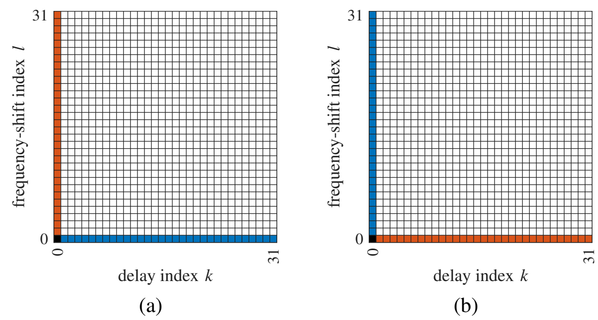

Fig. 1. Discrete ambiguity-function zeros and paths of SC-FDE and OFDM on the delay-frequency-shift grid. Black, white, orange, and blue cells indicate the origin, ambiguity-function zeros, nonzero points, and the selected path, respectively. (a) SC-FDE; (b) OFDM.

B. Examples

To illustrate the above concepts, we next analyze several representative waveform schemes, including SC-FDE, OFDM, OTFS, and AFDM.

For SC-FDE and OFDM, their prototype waveform vectors can be regarded as

$$g_{\text{SC-FDE}} = [1,0,\ldots,0], \qquad g_{\text{OFDM}} = [1,1,\ldots,1]. \tag{20}$$

Accordingly, their paths are

$$\mathcal{P}_i^{\text{SC-FDE}} = T_i M_0, \tag{21}$$

$$\mathcal{P}_i^{\text{OFDM}} = T_0 M_i. \tag{22}$$

By computing the ambiguity-function zeros of these two waveforms, we obtain the patterns shown in Fig. 1. In Figs. 1–4, the horizontal axis denotes the delay index and the vertical axis denotes the frequency-shift index. Black, white, orange, and blue cells indicate the origin, ambiguity-function zeros (orthogonal shifts), nonzero points (non-orthogonal shifts), and the selected path, respectively. In Fig. 1, the horizontal blue cells correspond to the SC-FDE path, whereas the vertical blue cells correspond to the OFDM path. Hence, SC-FDE constructs an orthogonal basis through time shifts of the prototype waveform, while OFDM does so through frequency shifts.

OTFS and AFDM are two popular waveform schemes for doubly selective channels. Unlike single-carrier and OFDM waveforms, both OTFS and AFDM can simultaneously handle multipath delay and Doppler frequency shift, and exhibit excellent performance in doubly selective channels.

OTFS is a two-dimensional modulation scheme whose key idea is to modulate information symbols in the delay-Doppler (DD) domain rather than in the traditional time-frequency (TF) domain. In doubly selective channels, the channel impulse response is typically sparse and slowly varying in the DD domain, which allows OTFS to effectively capture and exploit the channel characteristics, thereby achieving enhanced diversity gain and improved performance.

The modulation and demodulation of OTFS can be viewed as a transformation process among the DD domain, TF domain, and time domain. On the transmit side, OTFS signal generation mainly involves the following three key steps: (a)

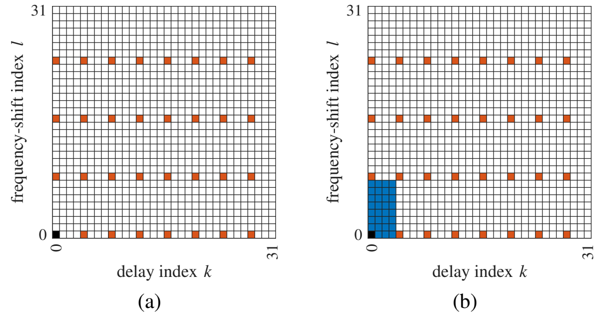

Fig. 2. OTFS waveform: (a) discrete ambiguity-function zeros; (b) corresponding path on the delay-frequency-shift grid.

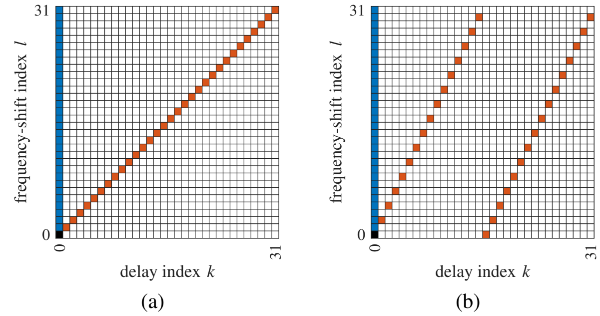

Fig. 3. AFDM waveform: discrete ambiguity-function zeros and paths for different c_1. (a) $c_1 = \frac{1}{2N}$; (b) $c_1 = \frac{2}{2N}$.

Information symbol mapping; (b) Inverse symplectic finite Fourier transform (ISFFT); (c) Heisenberg transform [9].

In fact, under the widely adopted rectangular transmit pulse and critical sampling condition $T\Delta f = 1$, the above procedure can be simplified as performing a discrete Fourier transform (DFT) along the N-dimension of the $N \times M$ symbol grid and then vectorizing along the M-dimension to form a serial time-domain sequence. In matrix form, the overall modulation can be written as [10]

$$\mathbf{s} = \left(\mathbf{F}_N^{\mathrm{H}} \otimes \mathbf{I}_M\right) \mathbf{K}\mathbf{x}, \tag{23}$$

where $\mathbf{F}_N$ denotes the N-point DFT matrix, $\mathbf{I}_M$ is the $M \times M$ identity matrix, and $\mathbf{K}$ is the commutation matrix satisfying $\mathrm{vec}(\mathbf{X}^{\mathrm{T}}) = \mathbf{K}\,\mathrm{vec}(\mathbf{X})$ for any $\mathbf{X} \in \mathbb{C}^{N\times M}$. Here $\mathbf{x} \in \mathbb{C}^{NM}$ denotes the vectorized DD-domain symbol vector and $\mathbf{s} \in \mathbb{C}^{NM}$ denotes the time-domain transmit vector. Moreover, (23) is a linear modulation matrix, so its columns are the basis waveforms. Under rectangular pulses and critical sampling, these columns can be interpreted as WH shifts of a sparse periodic prototype, which leads to (24) and (25).

From the Weyl-Heisenberg perspective, the prototype waveform of OTFS can be regarded as

$$g_{\mathrm{OTFS}} = [g_0, g_1, \ldots, g_{N-1}], \quad g_i = \begin{cases} 1, & \mathrm{mod}(i, M) = 0, \\ 0, & \mathrm{mod}(i, M) \neq 0. \end{cases} \tag{24}$$

Its path is

$$\mathcal{P}_i^{\mathrm{OTFS}} = T_{\mathrm{mod}\,(i,N)} M_{\lfloor i/M \rfloor}. \tag{25}$$

The discrete ambiguity-function zeros and the corresponding path of OTFS on the grid are shown in Fig. 2.

Although the path is not a straight line, the coordinate differences between any two points on the path still lie in the zero set of the discrete ambiguity function. Consequently, the waveforms generated along this path form an orthogonal communication system.

AFDM is another popular waveform for doubly selective channels. It can be viewed as a parameterized extension of the orthogonal chirp-division multiplexing (OCDM) scheme. AFDM modulation is based on the affine Fourier transform (AFT) and its discrete implementation. The discrete AFT is given by [5]

$$S(m) = \frac{1}{\sqrt{N}} \sum_{n=0}^{N-1} e^{-\mathrm{j}2\pi\left(c_1 n^2 + \frac{1}{N} mn + c_2 m^2\right)} s(n), \tag{26}$$

which involves two parameters c_1 and c_2. OCDM is a special case of AFDM with $c_1 = c_2 = \frac{1}{2N}$.

Let $\mathbf{s} = [s(0), s(1), \ldots, s(N-1)]^{\mathrm{T}}$ and $\mathbf{S} = [S(0), S(1), \ldots, S(N-1)]^{\mathrm{T}}$. The above expression can be written in matrix form as

$$\mathbf{S} = \mathbf{A}\mathbf{s} = \mathbf{\Lambda}_{c_2} \mathbf{F}_N \mathbf{\Lambda}_{c_1} \mathbf{s}, \tag{27}$$

where $\mathbf{A}$ is the discrete AFT matrix, while $\mathbf{F}_N$ is the unitary N-point DFT matrix and

$$\mathbf{\Lambda}_c = \mathrm{diag}\left(e^{-\mathrm{j}2\pi c n^2}, n = 0, 1, \ldots, N-1\right). \tag{28}$$

The work in [11] has shown that, for AFDM, system performance under different channel conditions is essentially independent of the parameter c_2. Hence we can set $\mathbf{\Lambda}_{c_2} = \mathbf{I}_N$, and AFDM modulation simplifies to

$$\mathbf{s} = \mathbf{\Lambda}_{c_1}^{\mathrm{H}} \mathbf{F}_N^{\mathrm{H}} \mathbf{S}. \tag{29}$$

Here $\mathbf{S} \in \mathbb{C}^N$ denotes the input symbol vector in the affine-Fourier domain and $\mathbf{s} \in \mathbb{C}^N$ denotes the time-domain transmit vector. Equation (29) shows that AFDM applies a chirp weighting to the IDFT basis, so the resulting waveform family can be interpreted as frequency shifts of a chirp prototype, which leads to (30) and (31).

From the Weyl-Heisenberg perspective, the prototype waveform of AFDM can be viewed as

$$g_{\mathrm{AFDM}}(n) = e^{-\mathrm{j}2\pi c_1 n^2}. \tag{30}$$

Its path is

$$\mathcal{P}_i^{\mathrm{AFDM}} = T_0 M_i. \tag{31}$$

For $c_1 = \frac{1}{2N}$ and $c_1 = \frac{2}{2N}$, the discrete ambiguity-function zeros and the corresponding paths are shown in Fig. 3.

IV. New Orthogonal Waveform Based on the Weyl-Heisenberg Framework

Building on the above WH-based orthogonal construction rule and the insights from existing schemes, we now design a new orthogonal waveform set tailored to doubly selective channels.

Compared with SC-FDE and OFDM, OTFS and AFDM spread their signal energy over both time and frequency rather than concentrating it in only one dimension. For doubly selective channels, this is desirable because it reduces reliance on a small subset of time samples or frequency bins, so

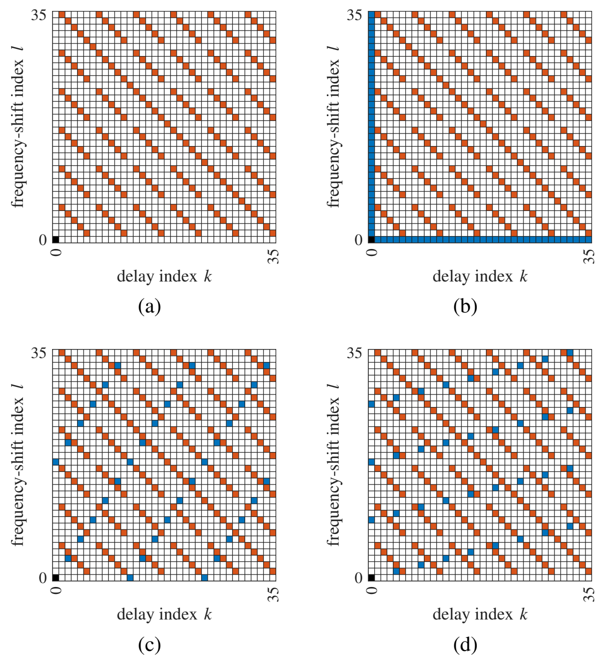

Fig. 4. Discrete ambiguity-function zeros and example paths that can form orthogonal basis of the proposed waveform. (a) discrete ambiguity-function zeros. (b) path: $p = 0, q = 1$ and $p = 1, q = 0$. (c) path: $p = 2, q = 3$. (d) path: $p = 4, q = 1$.

neither frequency-selective fading nor time selectivity is likely to dominate the effective signal energy. Although this does not by itself guarantee optimality, it provides a useful robustness criterion for prototype design.

From this viewpoint, a natural choice is a prototype with constant modulus in both the time and frequency domains. In the Weyl-Heisenberg framework, the basis signals are generated only through cyclic time shifts and frequency modulations. These operations preserve the prototype magnitude in time and correspond to phase rotations or cyclic shifts in frequency. Hence, if the prototype and its DFT are both constant-modulus, then all generated basis signals inherit the same balanced time-frequency spreading.

We propose a prototype waveform that satisfies these properties:

$$\mathbf{g} = \mathrm{vec}_{\mathrm{row}}\left[\left(\mathbf{F}_Q \cdot \mathrm{diag}(e^{\mathrm{j}\boldsymbol{\theta}})\right)^{\mathrm{T}}\right], \tag{32}$$

where $\mathbf{F}_Q$ denotes the Q-dimensional Fourier matrix, $\boldsymbol{\theta}$ is a real vector of length Q, and $\mathrm{vec}_{\mathrm{row}}[\cdot]$ denotes row-wise vectorization of a matrix.

The discrete ambiguity-function zeros of this vector are shown in Fig. 4a. Two obvious paths along which orthogonal basis can be constructed are

$$\mathcal{P}_i^A = T_i M_0, \tag{33}$$

$$\mathcal{P}_i^B = T_0 M_i. \tag{34}$$

In addition, for any path starting from the origin with slope p/q, if p and q have opposite parity, then each such path can also form an orthogonal basis, as illustrated in Fig. 4.

Let $\mathbf{x} \in \mathbb{C}^N$ denote a block of N data symbols to be transmitted. After passing through the waveform generation matrix $\mathbf{P} \in \mathbb{C}^{N\times N}$, the time-domain transmit signal becomes

$$\mathbf{s} = \mathbf{P}\mathbf{x}. \tag{35}$$

$$\begin{aligned} \mathbf{P} &= \left[\mathbf{p}_0, \mathbf{p}_1, \ldots, \mathbf{p}_{N-1}\right], \\ \mathbf{p}_i &= \mathcal{P}_i\, \mathbf{g},\ \ i = 0, 1, \ldots, N-1, \end{aligned} \tag{36}$$

where $\mathbf{g}$ is the prototype waveform and $\mathcal{P}_i$ denotes the ith WH operator in the path. With the chosen path, $\mathbf{P}$ is a unitary matrix.

To leverage existing results for block-transmission systems, a cyclic prefix (CP) is inserted so that the linear convolution of the channel can be represented as a cyclic convolution in matrix form. The received signal model is then

$$\mathbf{r} = \mathbf{H}\mathbf{s} + \mathbf{n} = \mathbf{H}\mathbf{P}\mathbf{x} + \mathbf{n}, \tag{37}$$

where $\mathbf{H} \in \mathbb{C}^{N\times N}$ is the time-domain channel matrix and $\mathbf{n}$ denotes additive noise.

For a time-invariant channel, the channel matrix becomes circulant due to the CP, so it can be diagonalized by the Fourier matrix. This greatly simplifies channel estimation and equalization in the frequency domain. In doubly selective fading, however, the effective channel matrix is generally non-circulant and cannot be diagonalized in a simple manner [12].

For a linear receiver, demodulation at the receiver performs the inverse processing of the transmitter. The estimated data vector can be written as

$$\hat{\mathbf{x}} = \mathbf{P}^{\mathrm{H}}\mathbf{G}\mathbf{r} = \mathbf{P}^{\mathrm{H}}\mathbf{G}\mathbf{H}\mathbf{P}\mathbf{x} + \mathbf{P}^{\mathrm{H}}\mathbf{G}\mathbf{n}, \tag{38}$$

where $\mathbf{G}$ is a linear equalization matrix.

Let $\mathbf{H}_{\mathrm{eq}} = \mathbf{H}\mathbf{P}$. For a linear MMSE equalizer with noise variance σ_n^2, where $\mathbb{E}[\mathbf{n}\mathbf{n}^{\mathrm{H}}] = \sigma_n^2\mathbf{I}_N$, we use

$$\mathbf{G}_{\mathrm{MMSE}} = \left(\mathbf{H}_{\mathrm{eq}}^{\mathrm{H}}\mathbf{H}_{\mathrm{eq}} + \sigma_n^2\mathbf{I}_N\right)^{-1}\mathbf{H}_{\mathrm{eq}}^{\mathrm{H}}. \tag{39}$$

V. Performance Simulation and Analysis

In this section, we evaluate and compare the BER performance of SC-FDE, OFDM, OTFS, AFDM, and the proposed waveform under different channel conditions via numerical simulations. All simulations are carried out under the following assumptions: (a) the carrier frequency is $f_c = 6$ GHz and the subcarrier spacing is $\Delta f = 15$ kHz; (b) QPSK modulation is employed; (c) all waveform schemes adopt block transmission with a block length of $N = 256$ and carry 256 QPSK symbols per block, ensuring a resource-fair comparison that differs only in the waveform-dependent precoder; for OTFS, this is realized through an $N_{\mathrm{OTFS}} \times M_{\mathrm{OTFS}}$ DD grid with $N_{\mathrm{OTFS}} = 8$ and $M_{\mathrm{OTFS}} = 32$; for the proposed waveform, we set $Q = 16$, so that $N = Q^2 = 256$; (d) a CP longer than the maximum delay spread is appended; (e) all waveform schemes use the same time-domain MMSE equalizer in (39), with only the waveform generation matrix $\mathbf{P}$ changed according to the waveform.

The AFDM parameter c_1 is selected according to the optimal values reported in [11] for the corresponding channel conditions. We additionally include two non-optimized settings for comparison: $c_1 = \frac{1}{2N}$ (corresponding to OCDM)

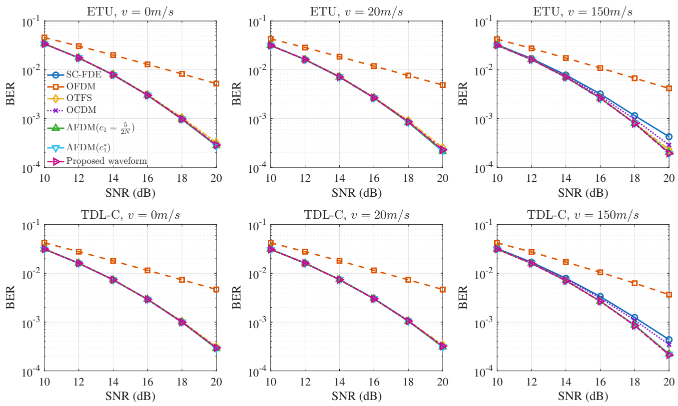

Fig. 5. BER performance comparison of different waveform schemes with an MMSE receiver under various channel conditions (LTE ETU and 5G TDL-C, $v = 0, 20, 150$ m/s).

and $c_1 = \frac{5}{2N}$. For the proposed waveform, the path is chosen as $\mathcal{P}_i = T_i M_0$ and the phase vector $\boldsymbol{\theta}$ is drawn once with i.i.d. entries uniformly distributed over $[0, 2\pi)$ and then kept fixed for all channel conditions and simulations.

Figure 5 shows the BER performance of different waveform schemes with an MMSE receiver under various channel conditions. The multipath delay and power profiles follow the Long-Term Evolution (LTE) extended typical urban (ETU) channel model and the 3GPP 5G tapped delay line model C (TDL-C), and the mobile speeds are set to $v = 0$ m/s (static), $v = 20$ m/s (typical vehicle), and $v = 150$ m/s (high-speed railway). The Doppler spectrum follows the classical Jakes' model. It can be observed that, in all simulated channel environments, OFDM exhibits the worst BER performance. This is because each OFDM symbol occupies only a narrow frequency bin and is therefore more vulnerable to deep fades in frequency-selective channels, whereas the other waveforms provide additional frequency spreading. When the mobile speed is low, all non-OFDM waveforms show similar performance. As the speed increases to the high-speed railway scenario, SC-FDE and OCDM (AFDM with $c_1 = \frac{1}{2N}$) both experience noticeable performance degradation. In contrast, OTFS, parameter-optimized AFDM, and the proposed waveform better balance the impacts of time-domain and frequency-domain fading, achieving superior BER performance and approaching the theoretical MMSE lower bound. These results demonstrate the effectiveness of the proposed waveform in doubly selective channels. In particular, its near-uniform time-frequency energy spreading provides an implicit averaging effect over both frequency selectivity and time variation, which helps maintain stable performance as the mobility increases.

VI. Conclusion

This paper proposed a unified waveform design framework for doubly selective channels based on the Weyl-Heisenberg (WH) framework. By representing time and frequency shifts as unitary WH operators and linking orthogonality to the ambiguity function and its zero set, we established a common perspective that interprets SC-FDE, OFDM, OTFS, and AFDM as different operator paths on the delay-frequency-shift grid. This unification clarifies their structural relationships and provides explicit criteria for constructing orthogonal waveform sets under a single mathematical framework. In addition, the proposed WH-based construction rule provides an explicit and reusable way to generate orthogonal waveform sets from ambiguity-function zeros, and the resulting constant-modulus prototype waveform yields a practical waveform that achieves BER performance comparable to OTFS and AFDM under MMSE reception in the considered doubly selective channels.

Acknowledgment

Harbin Institute of Technology's research is partially supported by the Key Program of the National Natural Science Foundation of China under Grant U23A20278. EURECOM's research is partially supported by its industrial members: ORANGE, BMW, SAP, iABG, Norton LifeLock, by the French PEPR-5G projects PERSEUS and YACARI, and by the EU H2030 RI project CONVERGE.

References

[1] International Telecommunication Union – Radiocommunication Sector (ITU-R), "Framework and Overall Objectives of the Future Development of IMT for 2030 and Beyond," ITU-R, Geneva, Switzerland, White Paper IMT-2030, 2023.

[2] C.-X. Wang, X. You, X. Gao, X. Zhu, Z. Li, C. Zhang, H. Wang, Y. Huang, Y. Chen, H. Haas, J. S. Thompson, E. G. Larsson, M. D. Renzo, W. Tong, P. Zhu, X. Shen, H. V. Poor, and L. Hanzo, "On the Road to 6G: Visions, Requirements, Key Technologies, and Testbeds," *IEEE Communications Surveys & Tutorials*, vol. 25, no. 2, pp. 905–974, 2023.

[3] J. Rodríguez-Piñeiro, Z. Wei, J. Wang, C. A. Gutiérrez, and L. M. Correia, "6G-Enabled Vehicle-to-Everything Communications: Current Research Trends and Open Challenges," *IEEE Open Journal of Vehicular Technology*, vol. 6, pp. 2358–2391, 2025.

[4] R. Hadani, S. Rakib, M. Tsatsanis, A. Monk, A. J. Goldsmith, A. F. Molisch, and R. Calderbank, "Orthogonal Time Frequency Space Modulation," in *2017 IEEE Wireless Communications and Networking Conference (WCNC)*, 2017, pp. 1–6.

[5] A. Bemani, N. Ksairi, and M. Kountouris, "Affine Frequency Division Multiplexing for Next Generation Wireless Communications," *IEEE Transactions on Wireless Communications*, vol. 22, no. 11, pp. 8214–8229, 2023.

[6] F.-M. Han and X.-D. Zhang, "Wireless multicarrier digital transmission via Weyl-Heisenberg frames over time-frequency dispersive channels," *IEEE Transactions on Communications*, vol. 57, no. 6, pp. 1721–1733, 2009.

[7] S. Gopalam, "General Delay-Doppler Domain Signalling using Periodic Discrete Weyl-Heisenberg Sets and Analog Twisted Convolution Filters," *TechRxiv*, vol. 2024, no. 0923, 2024.

[8] S. Bannert, K. Gröchenig, and J. Stöckler, "Discretized Gabor Frames of Totally Positive Functions," *IEEE Transactions on Information Theory*, vol. 60, no. 1, pp. 159–169, 2014.

[9] W. Yuan, S. Li, Z. Wei, Y. Cui, J. Jiang, H. Zhang, and P. Fan, "New delay Doppler communication paradigm in 6G era: A survey of orthogonal time frequency space (OTFS)," *China Communications*, vol. 20, no. 6, pp. 1–25, 2023.

[10] Q. Hua, L. Yun, S. Xiayang, Y. Hua, J. Fei, and C. Yinming, "OTFS on overspread doubly selective channel," *China Communications*, vol. 21, no. 11, pp. 205–215, 2024.

[11] Z. Li, C. Zhang, G. Song, X. Fang, X. Sha, and D. T. M. Slock, "Chirp Parameter Selection for Affine Frequency Division Multiplexing With MMSE Equalization," *IEEE Transactions on Communications*, vol. 73, no. 7, pp. 5079–5093, 2025.

[12] W. Benzine, A. Bemani, N. Ksairi, and D. Slock, "Models, Methods, and Waveforms for Estimation and Prediction of Sparse Time-Varying Channels," *IEEE Transactions on Wireless Communications*, vol. 25, pp. 9623–9638, 2026.